National Aeronautics and Space Administration

Orbital Debris
Quarterly News

Inside...

A publication of
the NASA Orbital
Debris Program Office

Two Anomalous Events in GEO

Summer 2017 was marred by two apparently anomalous events in the geosynchronous orbit (GEO) belt. Both incidents have been observed by commercial space situation awareness providers, but as of 26 December 2017 no debris from either event have entered the public catalog.

The GEO communications spacecraft AMC-9 (International Designator 2003-024A, U.S. Strategic Command [USSTRATCOM] Space Surveillance Network [SSN] catalog number 27820), formerly known as GE-12, experienced an energetic event estimated to have occurred at approximately 07:10 GMT on 17 June 2017, after approximately 14 years on-orbit. Fig. 1 depicts the orbital evolution of the spacecraft in 2017. SES, the spacecraft owner-operator, described this event as a "serious anomaly." Following this event, the spacecraft began a westward drift in the GEO belt. Debris fragments have been observed in the vicinity of the AMC-9 spacecraft. SES has regained control of the spacecraft and has transferred AMC-9 to the so-called graveyard orbit, a long-term disposal orbit region located above the GEO belt. The NASA Orbital Debris Program Office (ODPO) characterizes this episode as an anomalous event.

The spacecraft bus is the popular Thales Alenia Space (formerly Alcatel Space) Spacebus-3000B3

platform. Spacecraft dry mass is estimated to be on the order of 2000 kg. On-board stored energy sources include fuel and pressurized components, as well as the battery subsystem.

The Indonesian GEO communications spacecraft TELKOM-1 (1999-042A, SSN catalog number 25880) experienced an energetic event on or about 25 August 2017, after over 18.1 years on-orbit—3 years past its nominal operational lifetime. An examination of the Two Line Element data indicates an observable change in spacecraft orbit between 26 and 29 August. At the beginning of this time interval, approximately
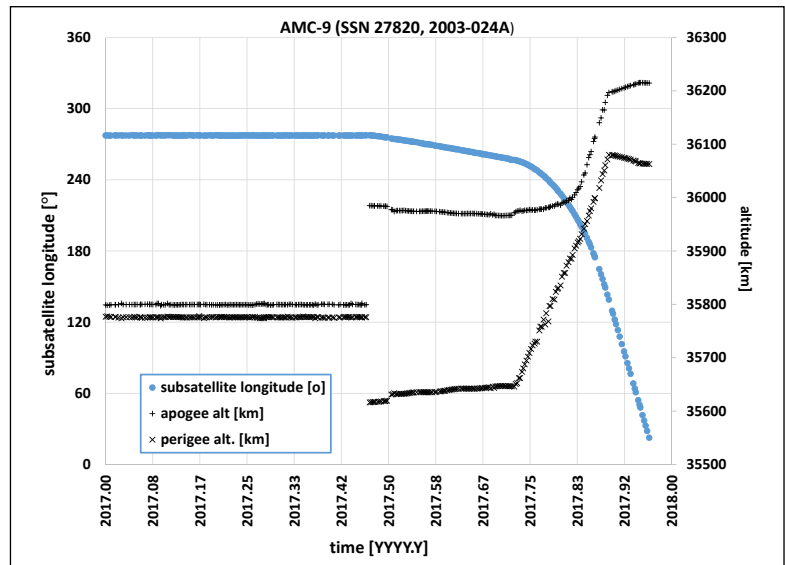
Figure 1. The 2017 orbital evolution of the AMC-9 spacecraft. Depicted are the subsatellite longitude, demonstrating a westward drift post-event, and the apogee/perigee altitude history. The altitude profile clearly indicates the abrupt nature of the 17 June 2017 event, recovery activities by the owner/operator, and the final boost to the so-called graveyard orbit above the GEO belt. Inclination control appears to have terminated in late June 2017.

Events in GEO
continued from page 1

TELKOM-1 (SSN 25880, 1999-042A)

Legend:
- subsatellite longitude [o]
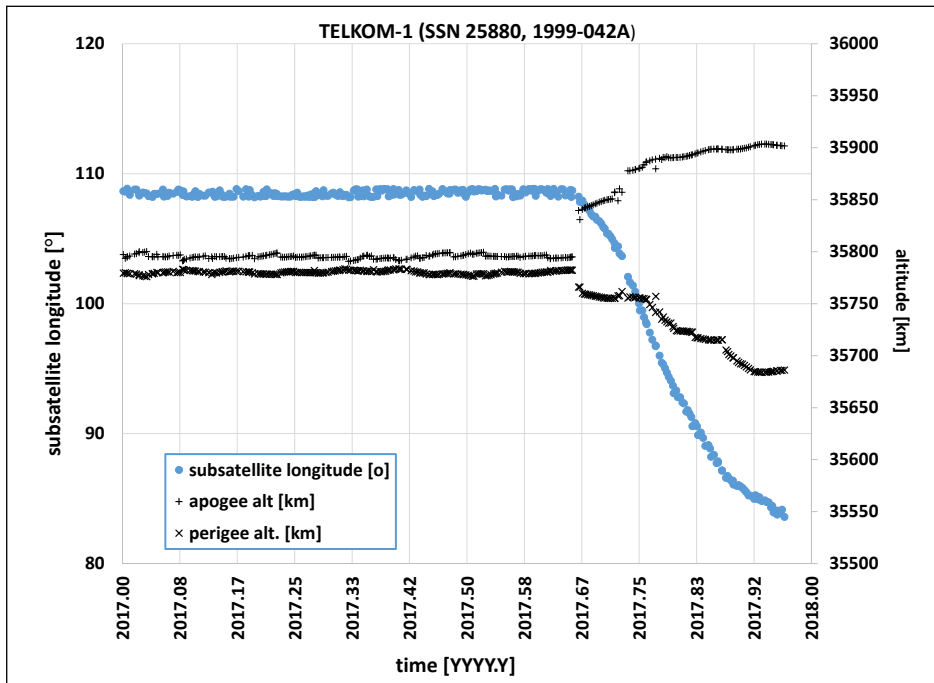- + apogee alt [km]
- × perigee alt. [km]

Figure 2. The 2017 orbital evolution of the TELKOM-1 spacecraft. Depicted are the subsatellite longitudes, demonstrating a westward drift post-event, and the apogee/perigee altitude history. The altitude profile clearly indicates the abrupt nature of the event and possible mitigation activities by the owner/operator. Inclination control apparently terminated in early September 2017.

10:43 GMT on 26 August, TELKOM-1 was in a 35793 x 35781 km, 0.0112° orbit; afterwards, at approximately 19:36 GMT on 29 August, the orbit was 35838 x 35764 km at an inclination of 0.0237°. PT Telkom, the spacecraft owner-operator, declared on 30 August that the spacecraft could not be salvaged [1]. Following this event, the spacecraft began a westward drift in the GEO belt. As this ODQN goes to press, the spacecraft orbit has evolved as depicted in Fig. 2. The NASA Orbital Debris Program Office (ODPO) characterizes this episode as an anomalous event.

The spacecraft bus is the Lockheed Martin A2100 platform. Spacecraft dry mass is estimated to be on the order of 1640 kg. On-board stored energy sources include fuel and pressurized components as well as the battery subsystem.

Reference
1. "Antenna glitch disconnects Telkom-1 satellite customers in Indonesia," http://spacenews.com/antenna-glitch-disconnects-telkom-1-satellite-customers-in-indonesia/ when accessed December 2017. ◆

Space Debris Sensor Launches Aboard SpaceX-13

The NASA Orbital Debris Program Office (ODPO) Space Debris Sensor (SDS) was launched to the International Space Station (ISS) aboard the Commercial Resupply mission CRS-13 (or SpaceX-13, SpX-13) vehicle on Friday, 15 December 2017, from Cape Canaveral Air Force Station's (CCAFS's) Launch Complex 40. Following the launch of a Space Exploration Technologies Corp. (SpaceX) Falcon 9 recoverable booster, Fig. 1, the Dragon vehicle separated from the Falcon 9's second stage, Fig. 2, *en route* to the ISS. The launch featured, for the first time, the second use of both the Falcon 9 first stage and the Dragon capsule, and post-staging the Falcon 9 first stage landed at SpaceX's Landing Zone 1 at CCAFS. The Dragon capsule rendezvoused with the ISS on Sunday, 17 December, and was captured and docked that day.

The SDS was robotically extracted from the SpX-13 Dragon trunk and installed on 1 January 2018. As seen in Fig. 3, the SDS is hosted

at the ESA Columbus module's External Payload Facility-Starboard Overhead-X (EPF-SOX)

location. Following a multi-week checkout period SDS is expected, as the ODQN goes to

press, to commence 3 years of operations at this location. Following completion of the SDS mission, the SDS is planned to be disposed of by reentry aboard a future CRS-series mission.

The SDS is the first flight demonstration of the Debris Resistive/Acoustic Grid Orbital NASA-Navy Sensor (DRAGONS) developed and matured by the NASA ODPO [1]. The DRAGONS concept combines several technologies to characterize the size, speed, direction, and density of small impacting objects. With a minimum 3-year operational lifetime, the SDS is anticipated to collect statistically significant information on orbital debris ranging from 50 μm to 500 μm in size. Most impacts will be around the threshold of 50 μm; the estimated number of 500 μm and larger impacts for a square meter in an ISS orbit over 2018-2020 is 0.84. The development of the SDS has been chronicled

SDS Launches

in the ODQN (ODQN vol. 21, Issue 3, August 2017, p. 2, "Update on the Space Debris Sensor" and pp. 3-6 "Benefits of a High LEO *In-situ* Measurement Mission"; ODQN vol. 21, Issue 1, February 2017, p. 1, "Space Debris Sensor Waiting for Launch" and pp. 9-10 "SDS is Readied for Flight" photo feature; ODQN vol. 19, Issue 2, April 2015, p. 11, "Space Debris Sensor (SDS) testing in progress at NASA White Sands Test Facility"; ODQN vol. 19, Issue 1, January 2015, pp. 2-3, "DRAGONS to Fly on the ISS"; ODQN

vol. 16, Issue 3, July 2012, pp. 2-3, "Development of DRAGONS-An MMOD Impact Detection Sensor System"). Readers are further directed to these online and social media resources:

• https://www.nasa.gov/mission_pages/station/research/news/sensor_to_monitor_orbital_debris_outside_ISS

• @**ISS_Research** (Twitter)

• https://www.youtube.com/watch?v=O0i7-xqRF0s (launch recap accessed 19 December 2017)

Reference

Hamilton, J., Liou, J.-C., Anz-Meador, P.D., *et al.*, "Development of the Space Debris Sensor," 7th European Conference on Space Debris, Darmstadt, Germany, published by ESA Space Debris Office (April 2017). ♦

Figure 1. The SpaceX Dragon spacecraft successfully launched to the International Space Station at 10:36 a.m. EST Dec. 15, 2017, from Cape Canaveral Air Force Station in Florida. Credits: NASA/Tony Gray and Sandra Joseph. Retrieved December 17 at https://www.nasa.gov/press-release/nasa-sends-new-research-to-space-station-aboard-spacex-resupply-mission .

Figure 2. The Dragon trunk following separation from the SpaceX Falcon 9 second stage; clearly visible are the trunk payloads SDS at the 9 o'clock position and the Total & Spectral solar Irradiance Sensor experiment at the 1 o'clock position. The Flight Releasable Attachment Mechanism station at the 5 o'clock position was flwn empty for this flight Credit: NASA
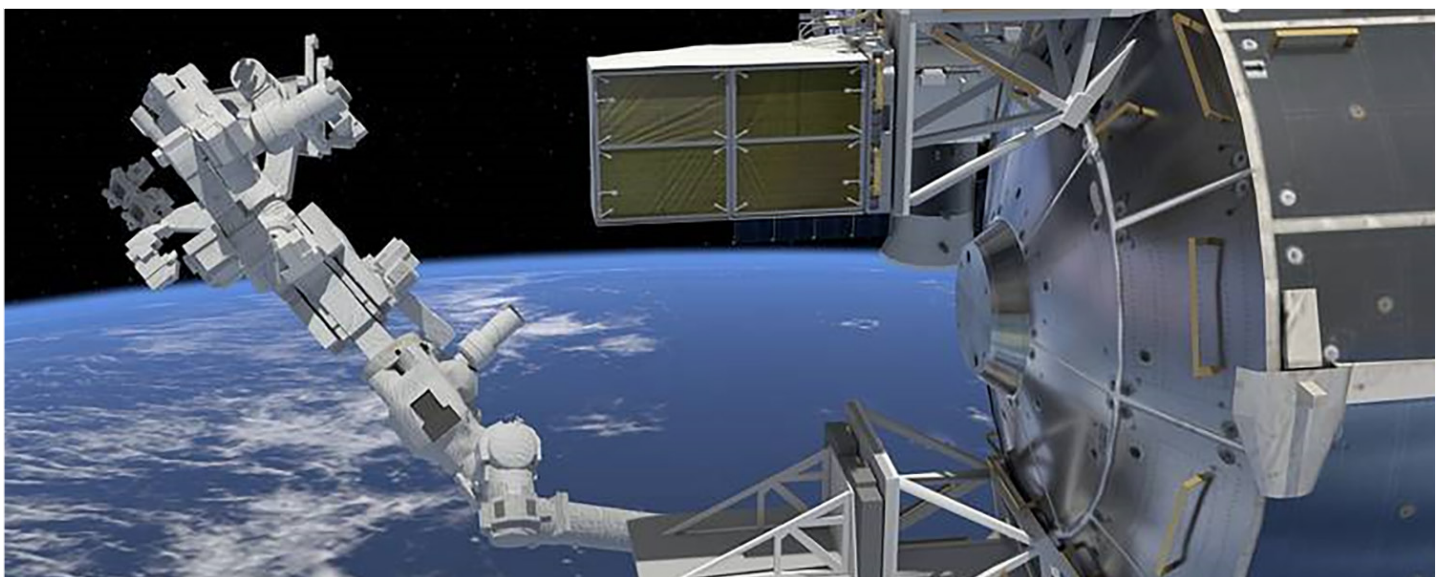

Figure 3. Having been installed robotically, in this artist's concept, the SDS resides at the ESA Columbus module's EPF-SOX location. Credit: NASA

PROJECT REVIEWS

SEM Analysis Results of Returned ISS PMA-2 Cover

J. HYDE, E. BERGER, D. LEAR, AND
E. CHRISTIANSEN

In a previous Orbital Debris Quarterly News (ODQN, vol. 20, issue 3, July 2016, pp. 4-6), we reported on results from post-flight inspection of the Pressurized Mating Adapter #2 (PMA-2) cover for micrometeoroid and orbital debris (MMOD) impacts [1, 2]. The PMA-2 cover was mounted on the forward-facing port of Node 2 which is the docking port that will by upcoming U.S. Commercial Crew vehicles. On 9 July 2013 a cover was installed to protect the exposed docking port. PMA-2 is located on the front of the ISS, with the cover facing directly into the velocity vector as shown in Fig. 1. The cover was removed in February 2015 during US EVA 30 (1.63 years exposure), and it was returned from ISS on SpaceX CRS-6 in May 2015. The cover consists of a beta cloth (Teflon coated fiberglass fabric) outer layer and internal layers of ballistic fabric.

A post-flight inspection of the returned space-exposed article revealed 26 sites with distinctive hypervelocity impact features. An idealized view of the approximately 2-m diameter cover with a surface area of 3.7 m^2 is provided in Fig. 2, along with the location of the 26 impact sites. Intact samples were extracted at six locations for additional imaging via Scanning Electron Microscopy (SEM) and chemical analysis using Energy Dispersive X-ray Spectroscopy (EDS). The table summarizes the EDS characterizations of the impactor types. Four of the six analyzed samples displayed indications of high density orbital debris as the source of the impact.

An example SEM image of the entry hole in the beta cloth outer layer for feature #1 is shown in Fig. 3. Higher magnification images of an area with impact melt containing iron-rich deposits are provided in Figs. 4 and 5. The spectra associated with the iron deposit are shown in yellow in Fig. 6, with spectra from clean beta cloth shown in red. Extraction of most remaining impact sites on the PMA-2 cover for SEM/EDS analysis is planned for 2018.

A comparison between the observed MMOD impact feature sizes and the expected number of MMOD features calculated by the computer code Bumper 3 is shown in Fig. 7. The 26 individual observations of entry hole size are depicted as yellow circles in the figure. There is good comparison, down to a limiting size of approximate 300 μm, between the observed holes in the cover and results of the Bumper 3 calculations for the number of entry holes in

PMA-2 beta cloth of various diameters, shown in solid lines for MEM-R2 and ORDEM 3.0 and with a dashed line for the MMOD total.

References

1. Hyde, J., Read, J., Lear, D., Christiansen, E. "MMOD Impacts Found on a Returned ISS Cover," Orbital Debris Quarterly News, vol. 20, issue 3, (July 2016).

2. Hyde, J., Christiansen, E., Lear, D., Nagy, K., Berger, E. "Surveys of Returned ISS Hardware for MMOD Impacts," 7th European Conference on Space Debris, Darmstadt, Germany, published by ESA Space Debris Office (April 2017).   ♦

PMA-2 Cover SEM/EDS Results

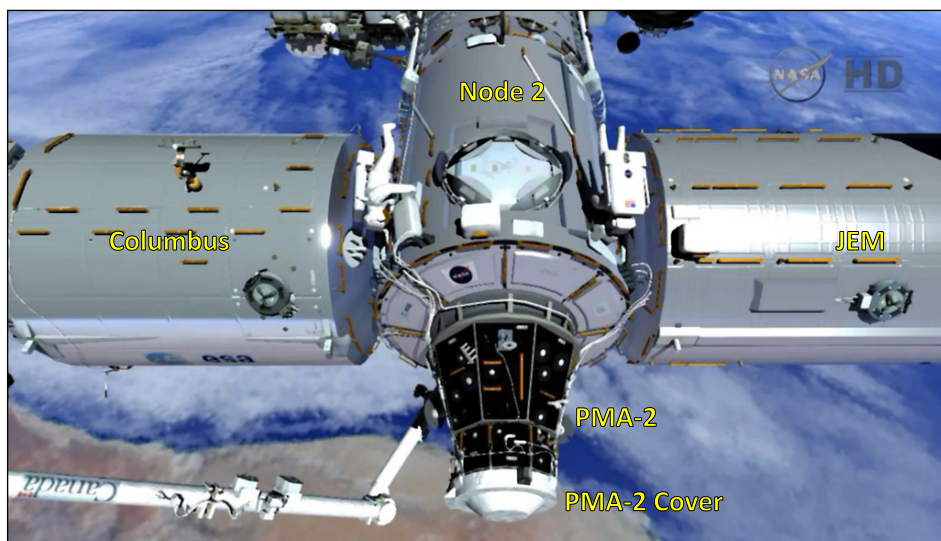| Feature #	Hole Diameter (mm)	Impactor Type/ Major Constituent	Possible Impactor
1	0.60	OD: Zn, S, Fe, Ti	Steel
2	1.01	OD: Ni	Steel
10	0.80	OD: Fe	Steel
12	0.57	MM: Ca, Mg, Fe, S	Chondrite
13	0.73	MM: Fe, Ni, S	Metal/sulfide-rich MM
24	0.36	OD: Fe, Ti	Steel

Figure 1. Location of PMA-2 cover. Source: NASA TV
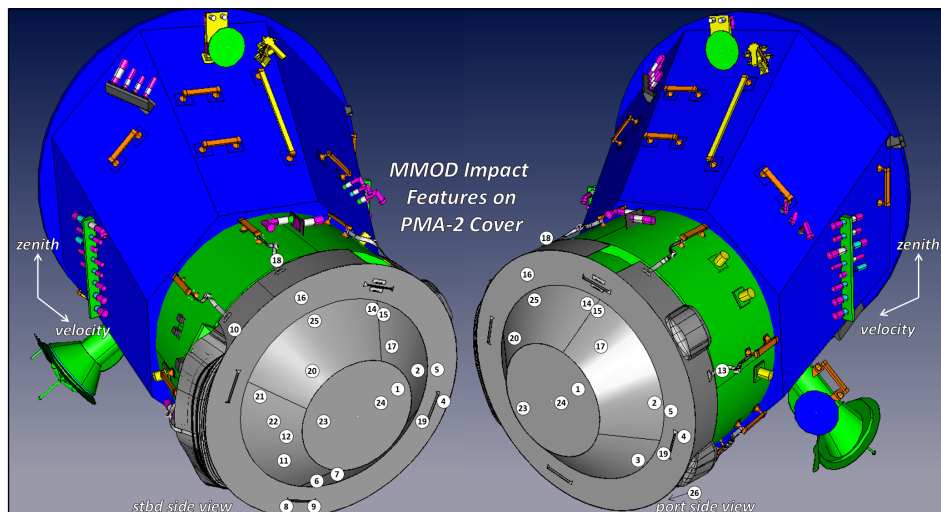

Figure 2. Port and starboard views of MMOD impact observations on PMA-2 cover. Source: NASA HVIT

SEM Analysis Results
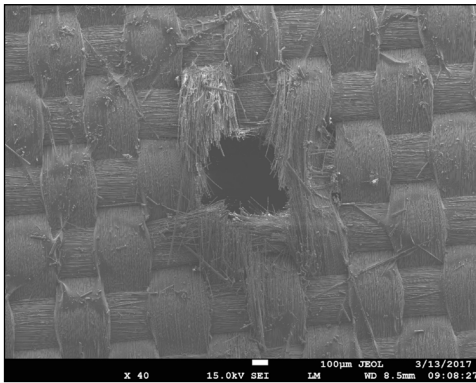
continued from page 4

Figure 3. Impact #1 - SEM imagery of damage on first layer (beta cloth). Source: NASA e-beam lab
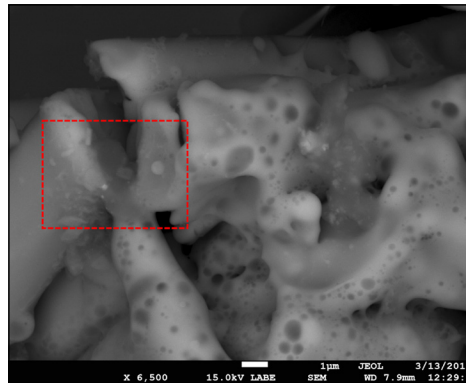

Figure 4. Impact #1 – SEM imagery of melted beta cloth components and iron rich deposits on first layer (beta cloth) fibers. Highlighted area shown in Fig. 5. Source: NASA e-beam lab
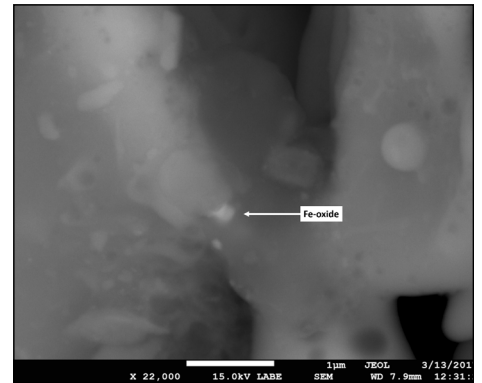
Figure 5. Impact #1 – Detail of iron oxide indication on first layer (beta cloth) fibers. Source: NASA e-beam lab
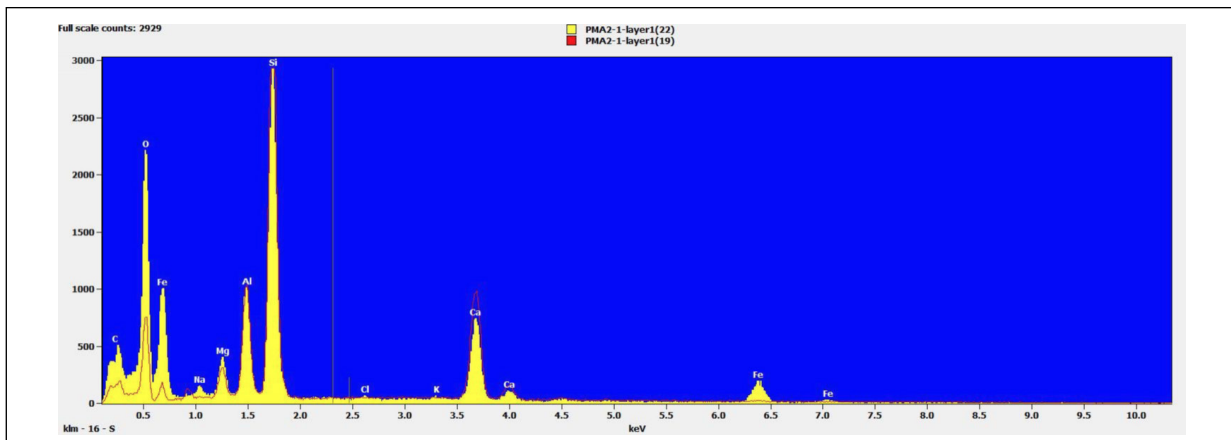

Figure 6. Impact # 1 – Spectra associated with iron oxide and Teflon on first layer (beta cloth) fibers shown in yellow. Clean beta cloth fiber spectra shown in red.   Source: NASA e-beam lab
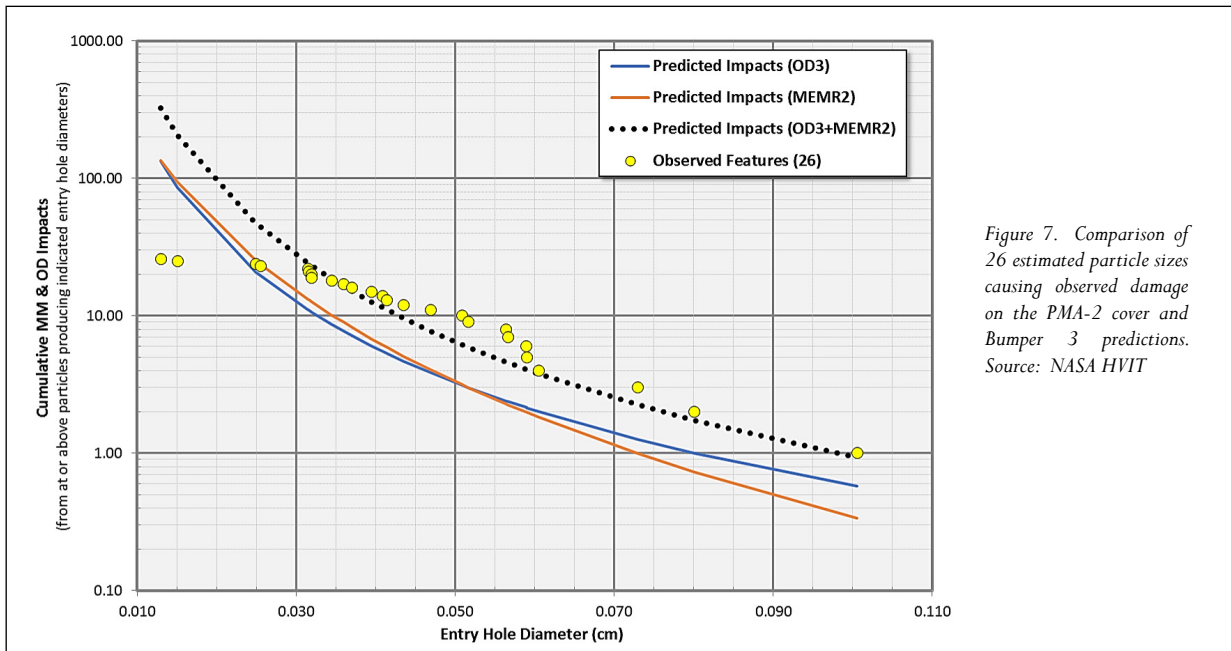

Figure 7. Comparison of 26 estimated particle sizes causing observed damage on the PMA-2 cover and Bumper 3 predictions. Source: NASA HVIT

CubeSat Study Project Review

D. VAVRIN AND A. MANIS

The NASA Orbital Debris Program Office has conducted a series of low Earth orbit (LEO) to geosynchronous orbit (GEO) Environment Debris (LEGEND) model computations to investigate the long-term effects of adding CubeSats to the environment. These results are compared to a baseline "business-as-usual" scenario where launches are assumed to continue as in the past without major CubeSat deployments. Using these results, we make observations about the continued use of the 25-year rule and the importance of the universal application of post-mission disposal (PMD).

The baseline population in this study depicts a future environment without the introduction of cluster deployments of CubeSats [1]. Actual historical launches and evolution from 1957 through 2014 are simulated as the initial condition for future traffic projection, which runs for 200 years starting in 2015. Future launches repeat the historical launch traffic cycle from 2007 to 2014 inclusive. The rate of future explosions is set to zero, assuming 100% passivation in the future projection, and the mission lifetime for payloads is set at 8 years. A specified percentage of spacecraft and rocket bodies are repositioned in decay orbits following PMD maneuvers, where they will re-enter the atmosphere within 25 years. The baseline population is projected using two PMD success rates of 60% and 90%. Each simulation includes 100 Monte Carlo runs to ensure a thorough statistical sampling of the future environment. Results shown are averages over
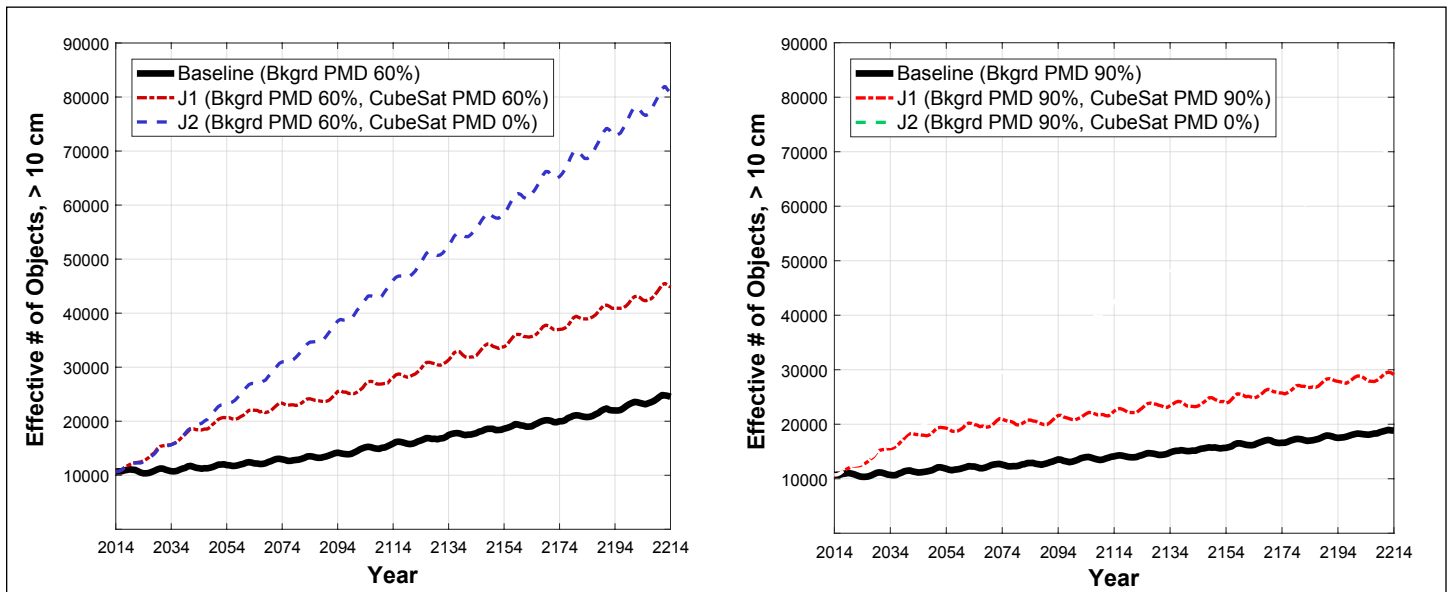
Figure 1. Effective number of objects in LEO, ≥10 cm, over 200-year projection with (1a, left) PMD success rate of 60%, and (1b, right) PMD success rate of 90%, baseline and scenarios J1 and J2. Note the steeper growth for scenario J2, where only non-CubeSats observe PMD, of both background and CubeSats.
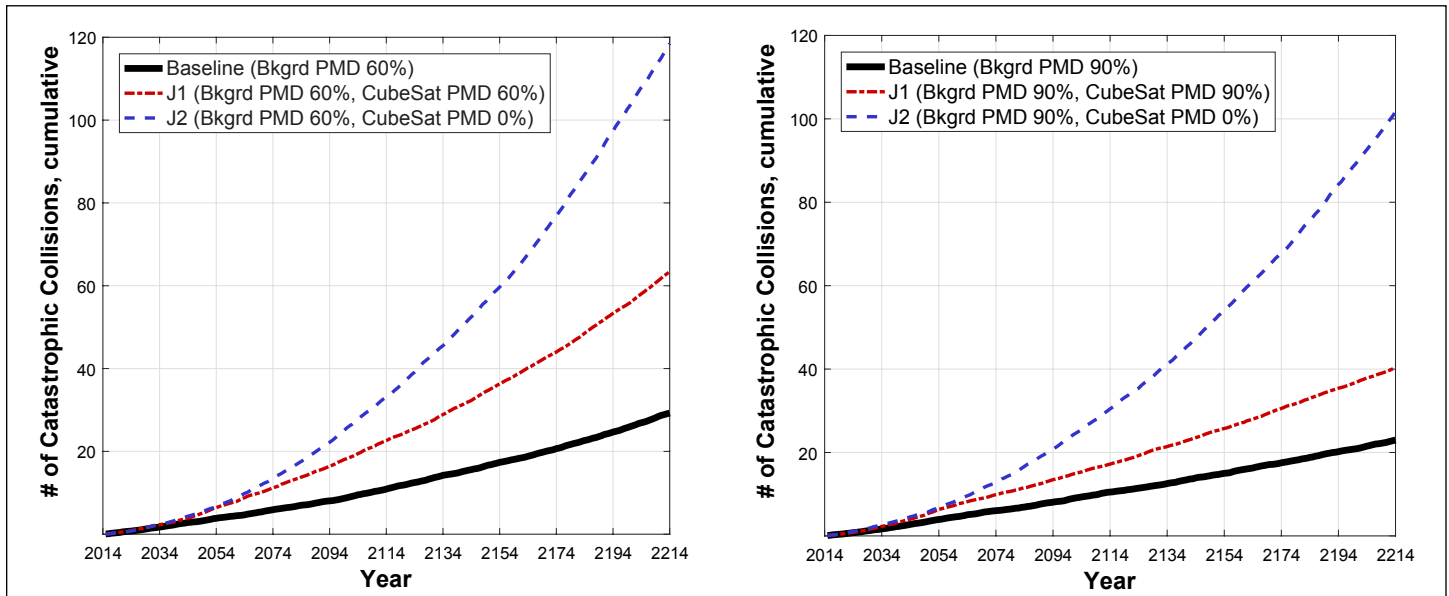

Figure 2. Cumulative number of catastrophic collisions in LEO over 200-year projection with (2a, left) PMD success rate of 60%, and (2b, right) PMD success rate of 90%, scenarios J1 and J2 compared to baseline.

CubeSat Study

continued from page 6

all Monte Carlo runs. Only objects ≥10 cm are considered for collision assessment in this study.

The CubeSat traffic scenarios use the same initial conditions and launch traffic cycle for regular intact objects as the baseline scenario, and additionally deploy CubeSats (1U, 3U, and 6U configurations) from a small satellite deployment system in the LEO region (200 km to 2000 km altitude). The mission lifetime of each CubeSat deployed in LEO is assumed to be 2 years for all future scenarios, during which time each CubeSat will apply its own set of collision avoidance maneuvers. After its mission lifetime, the CubeSat is placed in a post-mission disposal orbit where it will decay within 25 years with a 0%, 60%, or 90% probability of success. This study makes the following assumptions: 1) there are no launch failures or explosions of any CubeSats in the future environment, 2) the deployment system can support the launch of hundreds of CubeSats at a given time, and 3) each CubeSat does not perform any collision avoidance once in a PMD orbit.

In scenario J1, CubeSats are deployed from the 600 − 1000 km altitude range and have PMD success rates of 60% and 90%, the same PMD rate of regular intacts. Scenario J2 follows the same scheme as scenario J1, except the deployed CubeSats do not follow any post-mission disposal compliance (0% PMD success rate for CubeSats).

Figs. 1a and Fig. 1b show the growth of the effective number of objects over the 200-year projection for baseline (solid black line), J1 (blue dash-dot line), J2 (purple dashed line) with PMD compliance rates of 60% and 90%, respectively. Notice how setting the PMD rate to 0% substantially increases the total number of objects in the future environment. All three scenarios exhibit the same sharp rate of growth until 2043, the year when CubeSats launched in 2016 begin to be removed from the environment after their 25-year PMD decay orbit expires. After this point, the rate of object growth slows for scenario J1 to approximately match that of the baseline population. However, scenario J2 exhibits a steady rise in the effective number of objects over the full 200 years due to the lack of PMD for CubeSat intacts. The growth of CubeSats in this case swamps the beneficial effects of other satellites observing the 25-year rule.

The cumulative number of catastrophic collisions (*i.e.*, projectile energy-to-target mass ratio exceeds 40 J/g) in scenarios J1 and J2 over the 200-year projection with a PMD compliance rate of 60% is shown in Fig. 2a, while Fig. 2b illustrates the PMD 90% case. As realized with

the effective number of objects, increasing the PMD compliance rate from 60% to 90% for spacecraft and rocket bodies, while setting PMD rate for CubeSats to zero as in scenario J2, still yields a significant increase in the overall number of catastrophic collisions over the 200-year projection.

In the background population, collision fragments remain steady over future projection periods for both PMD cases. However, the CubeSat-related collisions comprise the majority of the number of catastrophic collisions. It is once again clear that scenario J2, with no PMD applied to CubeSats, produces the worst outcome − an increase in the cumulative number of catastrophic

collisions by more than a factor of 4 over the baseline population. A breakdown of the number of catastrophic collisions by altitude shows that this significant increase from the baseline population occurs at mid-LEO altitudes, around 600 − 1000 km, as seen in Fig. 3 for both 60% and 90% PMD compliance rates.

The effectiveness of PMD applied to CubeSats in addition to other payloads is evidenced by the significant difference in effective number of objects and cumulative catastrophic collisions seen between scenarios J1 (CubeSat PMD success rates of 60% and 90%) and J2 (0% PMD for CubeSats).
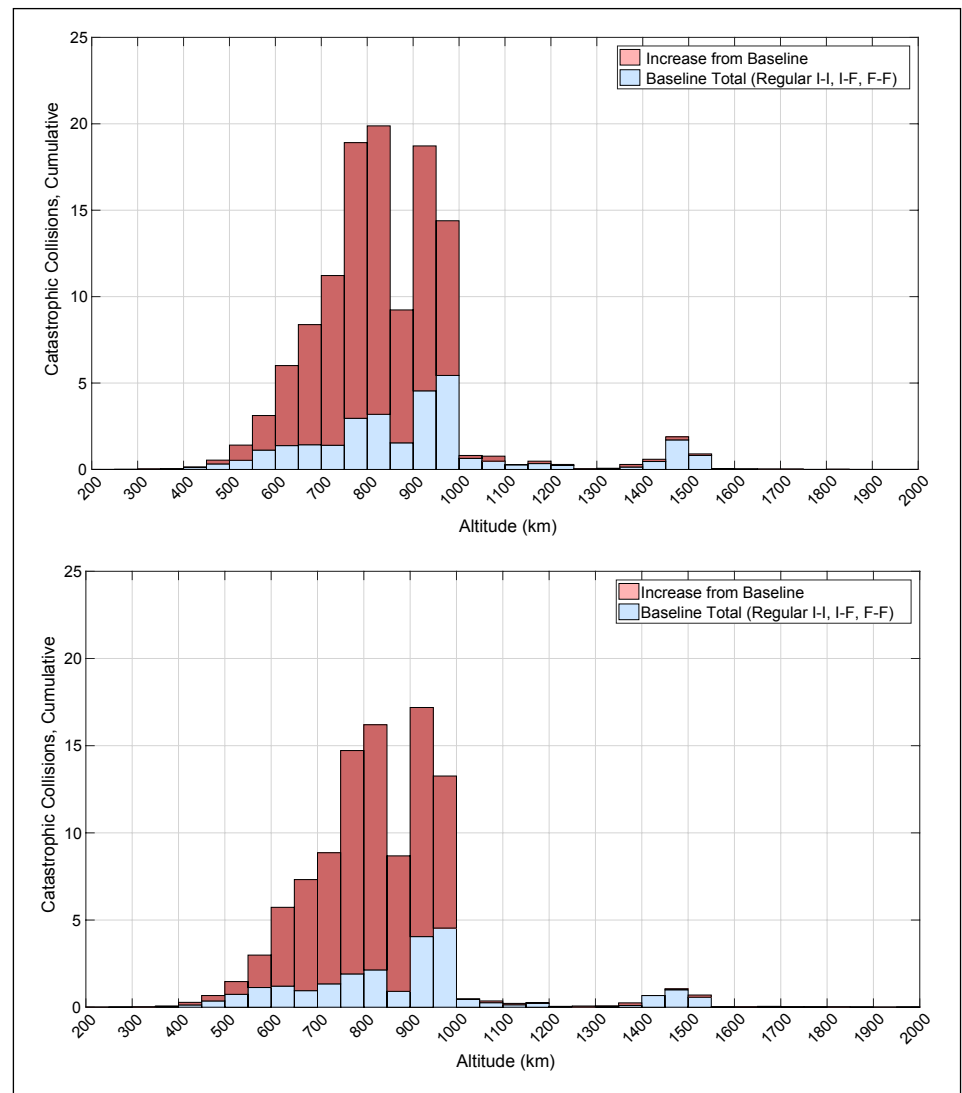
Figure 3. Increase in cumulative number of collisions from baseline population, by altitude (200 − 2000 km, 50 km bins) at the end of 200-year projection for Scenario J2 with (2a, top) PMD compliance rate of 60% and (2b, bottom) PMD compliance rate of 90% (0% PMD for CubeSats in both cases). Note that the number of collisions in each altitude bin is an average over 100 Monte Carlo runs.

CubeSat Study

Therefore, it is recommended that CubeSats follow the same 25-year rule as other payloads in order to avoid deterioration of mid-LEO altitudes (approximately 600-1000 km). At this time, it is not recommended that CubeSats be required to observe a different PMD standard than that applied to their larger cousins; specifically the 25-year rule. While PMD capabilities for small satellites still are under development, the outcomes of this study indicate that such technology is critical for successful long-term use of satellites in near-Earth space.

Reference

1. Matney, M., Vavrin, A., Manis, A. "Effects of CubeSat Deployments in Low-Earth Orbit," 7th European Conference on Space Debris, Darmstadt, Germany, published by ESA Space Debris Office, (17 April 2017). ♦

Space Debris Sensor Installation

The NASA Orbital Debris Program Office (ODPO) Space Debris Sensor (SDS) was robotically extracted from the SpX-13 Dragon trunk and installed on 1 January 2018. This photo feature documents the install process for readers and recognizes the NASA ROBO team for a successful installation of SDS aboard the International Space Station (ISS) *Columbus* module.

Figure 1 is a view, taken by an ISS truss-mounted camera, of the ISS Mobile Servicing System's Special Purpose Dextrous Manipulator (SPDM) reaching into the SpX-13 Dragon trunk to initiate the demate process from the trunk. Figure 2, taken from an SPDM camera, depicts the SPDM's Orbital Replacement Unit/Tool Changeout Mechanisms (OTCMs) entering the trunk. The SDS is visible at approximately the 7 o'clock position in the trunk.

In Figure 3 the SPDM OTCM has grasped the SDS payload adapter's microfixture and is in transit from the SpX-13 trunk to the *Columbus* module. From this position the SPDM would "hover" the SDS over the ESA *Columbus* module's External Payload Facility-Starboard Overhead-X (EPF-SOX) location prior to soft and hard docks on the EPF. Figure 4 completes this installation sequence as the SDS is firmly attached to the EPF-SOX platform and the OTCM is preparing to back away and on to perform ROBO's next task for the day. ♦

Figure 1. SPDM reaches into the SpX-13 Dragon trunk to extract SDS.

Figure 2. The SPDM OTCM enters the Dragon trunk.

Figure 3. The SPDM, with SDS, in transit to the Columbus EPF-SOX location.
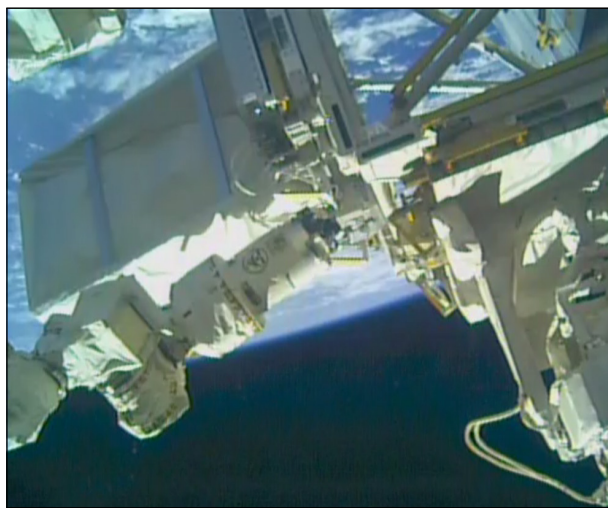

Figure 4. SDS installed on the EPX-SOX platform; SPDM OTCM preparing to detach and walk away.

UPCOMING MEETINGS

25-27 June 2018: 5th International Workshop on Space Debris Modeling and Remediation, Paris, France

CNES Headquarter will host the 5th Workshop on Space Debris Modeling and Remediation. Topics are anticipated to include, but are not necessarily limited to, modeling, including specificities coming from small satellites and constellations; high level actions and road-maps associated with debris remediation; remediation system studies, including those relative to small debris; design of specific concepts, including new ideas relative to just-in-time collision avoidance and proposals devoted to large constellations and small satellites; concepts derived from current space tugs initiatives; GNC aspects, rendezvous sensors and algorithms, de-spin, control during de-boost; and policy, economics, insurance, intellectual property, national security, and international cooperation aspects of debris remediation. The abstract submission deadline is 15 March 2018. Additional information about the conference, limited to 130 participants, is available from the ODQN editorial team.

14-22 July 2018: COSPAR 2018, Pasadena, CA, USA

The 42nd Assembly of the Committee on Space Research (COSPAR) Scientific will convene in the Pasadena Convention Center on Saturday, 14 July 2018 and run through Sunday, 22 July. This assembly marks the 60th year of COSPAR. The COSPAR panel Potentially Environmentally Detrimental Activities in Space (PEDAS) will conduct a program entitled "Space Debris – Providing the Scientific Foundation for Action." PEDAS.1 sessions will include advances in ground- and space-based measurements of the orbital debris environment, micrometeoroid and orbital debris environment modeling, risk assessment, mitigation and remediation, hypervelocity impact range developments, and protection. The abstract submission deadline is 9 February 2018. Please see the COSPAR website at https://cosparhq.cnes.fr/content/cospar-2018 and the Assembly website http://cospar2018.org/ for further information.

4-9 August 2018: 32nd Annual Small Satellite Conference, Logan, UT, USA

Utah State University (USU) and the AIAA will sponsor the 32nd Annual AIAA/USU Conference on Small Satellites at the university's Logan campus, Utah, USA. With the theme of "Delivering Mission Success," the 32nd conference will explore new technologies, design methods, processes, operational constructs, and activities that enhance the probability of success for small satellite missions. Session topics include assuring the space ecosystem, which will emphasize the interplay of small satellites and mission success to the sustainability of space, space situational awareness, space traffic management, and licensing and regulation. The abstract submission deadline is 8 February 2018. Additional information about the conference is available at https://www.smallsat.org .

11-14 September 2018: 19th Advanced Maui Optical and Space Surveillance Technologies Conference, Maui, Hawaii (USA)

The technical program of the 19th Advanced Maui Optical and Space Surveillance Technologies Conference (AMOS) is anticipated to focus on subjects that are mission critical to Space Situational Awareness. The technical sessions include papers and posters on Orbital Debris, Space Situational Awareness, Adaptive Optics & Imaging, Astrodynamics, Non-resolved Object Characterization, and related topics. Additional information about the conference is available at https://amostech.com and this announcement will be updated in the ODQN as details become available.

1-5 October 2018: 69th International Astronautical Congress (IAC), Bremen, Germany

The IAC will convene in Bremen in 2018 with a theme of "IAC 2018 – involving everyone." The IAA will organize the 16th Symposium on Space Debris as session A6 during the congress. Nine dedicated sessions are planned to cover all aspects of orbital debris activities, including measurements, modeling, hypervelocity impact, mitigation, remediation, and policy/legal/economic challenges for environment management. An additional joint session with the section C1.7 Astrodynamics will be conducted. The abstract submission deadline is 28 February 2018. Additional information for the 2018 IAC is available at: https://www.iac2018.org/ .

Monthly Number of Objects in Earth Orbit by Object Type

Number of Objects (Y-axis, 0 to 19000)

Year (X-axis, 1956 to 2018)

Legend:
- Total Objects
- Fragmentation Debris
- Spacecraft
- Mission-related Debris
- Rocket Bodies
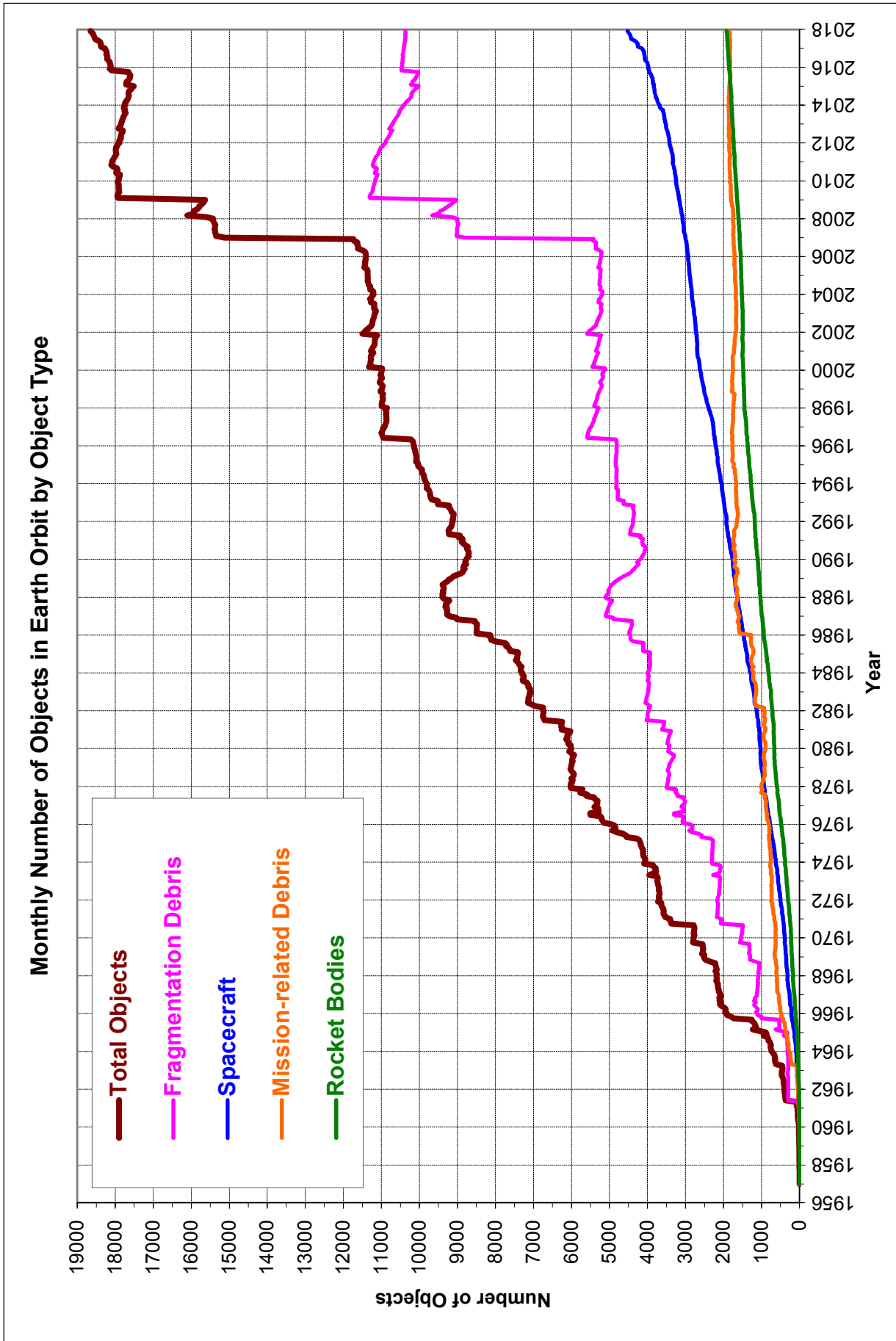
Monthly Number of Cataloged Objects in Earth Orbit by Object Type: This chart displays a summary of all objects in Earth orbit officially cataloged by the U.S. Space Surveillance Network. "Fragmentation debris" includes satellite breakup debris and anomalous event debris, while "mission-related debris" includes all objects dispensed, separated, or released as part of the planned mission.

Monthly Mass of Objects in Earth Orbit by Object Type

Legend:
- Total Objects
- Spacecraft
- Rocket Bodies
- Fragmentation Debris
- Mission-related Debris

X-axis: Year (1956–2018)
Y-axis: Mass in Orbit (metric tons) (0.0–9000.0)
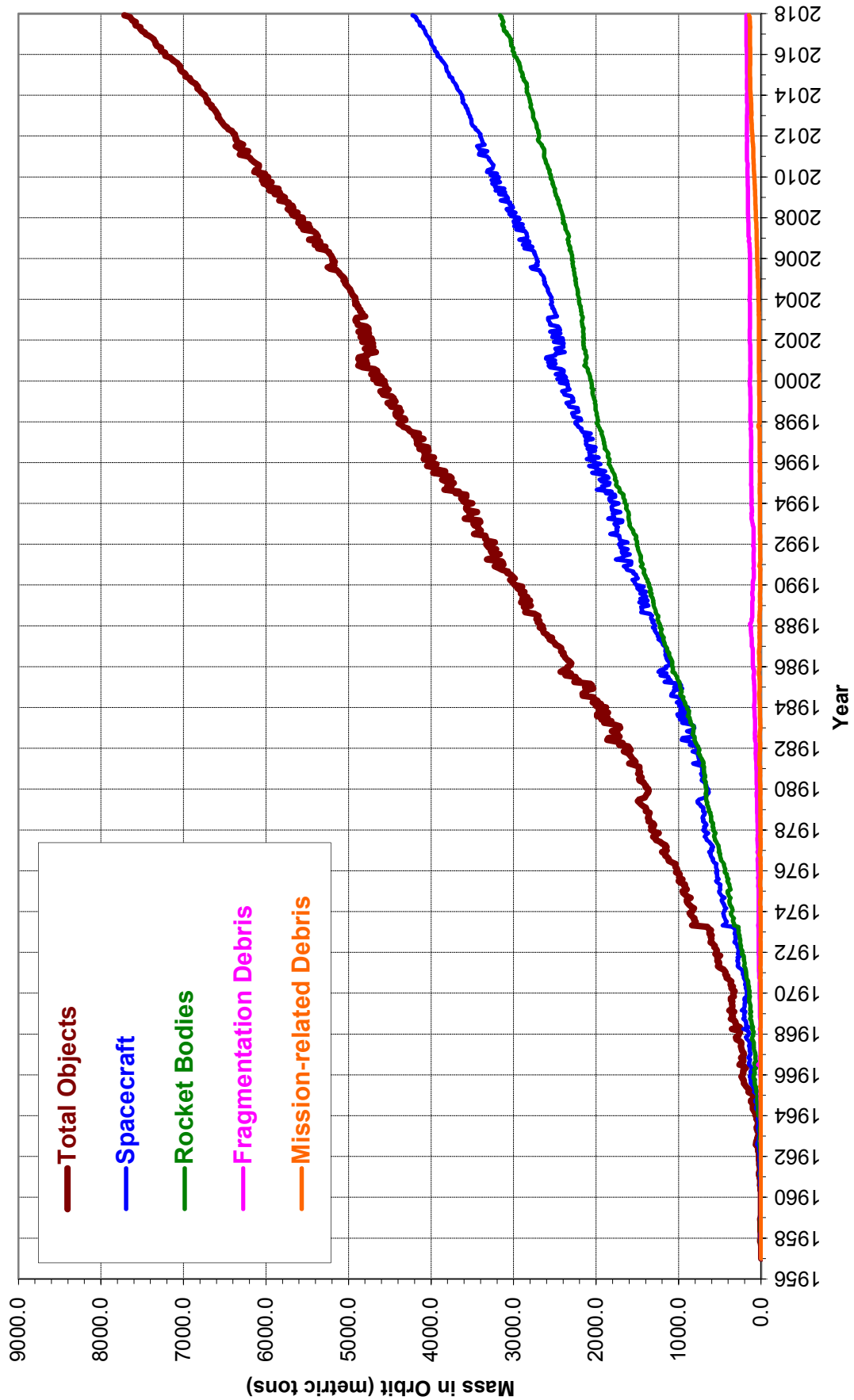
Monthly Mass of Objects in Earth Orbit by Object Type: This chart displays the mass of all objects in Earth orbit officially cataloged by the U.S. Space Surveillance Network.

SATELLITE BOX SCORE

(as of 04 January 2018, cataloged by the U.S. SPACE SURVEILLANCE NETWORK)

Country/ Organization	Payloads*	Rocket Bodies & Debris	Total
CHINA	269	3594	3863
CIS	1515	5003	6518
ESA	81	56	137
FRANCE	63	483	546
INDIA	85	115	200
JAPAN	170	100	270
USA	1634	4687	6321
OTHER	866	114	980
TOTAL	4683	14152	18835

* active and defunct

Visit the NASA
Orbital Debris Program Office
Website
www.orbitaldebris.jsc.nasa.gov

INTERNATIONAL SPACE MISSIONS
01 October 2017 – 31 December 2017

International Designator	Payloads	Country/ Organization	Perigee Altitude (KM)	Apogee Altitude (KM)	Inclination (DEG)	Earth Orbital Rocket Bodies	Other Cataloged Debris
2017-060A	VRSS–2	VENEZUELA	628	656	98.0	0	0
2017-061A	IRIDIUM 133	USA	776	780	86.4	0	0
2017-061B	IRIDIUM 100	USA	776	779	86.4		
2017-061C	IRIDIUM 122	USA	776	780	86.4		
2017-061D	IRIDIUM 129	USA	776	780	86.4		
2017-061E	IRIDIUM 119	USA	776	780	86.4		
2017-061F	IRIDIUM 107	USA	776	779	86.4		
2017-061G	IRIDIUM 132	USA	776	779	86.4		
2017-061H	IRIDIUM 136	USA	776	779	86.4		
2017-061J	IRIDIUM 139	USA	776	779	86.4		
2017-061K	IRIDIUM 125	USA	776	779	86.4		
2017-062A	QZS–4	JAPAN	32621	38948	40.5	1	0
2017-063A	ECHOSTAR 105/SES 11	SES	35785	35789	0.0	1	0
2017-064A	SENTINEL 5P	ESA	826	828	98.7	1	0
2017-065A	PROGRESS MS-07	RUSSIA	402	406	51.6	1	0
2017-066A	USA 279	USA	NO ELEMENTS AVAILABLE			0	0
1998-067NE	KESTREL EYE 2M	USA	398	403	51.6	0	0
1998-067NF	SIMPL	USA	400	404	51.6		
2017-067A	KOREASAT 5A	SOUTH KOREA	35783	35791	0.0	1	0
2017-068A	SKYSAT C11	USA	501	523	97.4	1	1
2017-068B	SKYSAT C10	USA	500	521	97.4		
2017-068C	SKYSAT C9	USA	500	505	97.4		
2017-068D	SKYSAT C8	USA	499	525	97.4		
2017-068E	SKYSAT C7	USA	498	524	97.4		
2017-068F	SKYSAT C6	USA	493	511	97.4		
2017-068J	FLOCK 3M 1	USA	499	524	97.3		
2017-068K	FLOCK 3M 3	USA	499	523	97.3		
2017-068L	FLOCK 3M 4	USA	499	522	97.4		
2017-068M	FLOCK 3M 2	USA	500	520	97.4		
2017-069A	BEIDOU–3 M1	CHINA	21507	21548	55.0	2	0
2017-069B	BEIDOU–3 M2	CHINA	21508	21548	55.0		
2017-070A	MOHAMMED VI–A	MOROCCO	638	640	98.0	0	0
2017-071A	CYGNUS 0A-8 &14 additional CubeSats	USA	373	393	51.6	1	2
2017-072A	FENGYUN 3D	CHINA	825	828	98.7	1	0
2017-072B	HEAD–1	CHINA	795	811	98.7		
2017-073A	JPSS 1	USA	826	828	98.7	0	0
2017-073B	BUCCANEER RMM	AUSTRALIA	458	821	97.7		
2017-073C	MIRATA	USA	454	820	97.7		
2017-073D	MAKERSAT 0	USA	452	820	97.7		
2017-073E	AO–91	USA	452	820	97.7		
2017-073F	EAGLESAT 1	USA	452	820	97.7		
1998-067NG	ECAMSAT	USA	398	405	51.6	0	0
1998-067NH	ASTERIA	USA	399	402	51.6		
1998-067NJ	DELLINGR (RBLE)	USA	400	403	51.6		
1998-067NK	TECHEDSAT 6	USA	386	390	51.6		
1998-067NL	OSIRIS-3U	USA	395	400	51.6		
2017-074A	JILIN-01-04	CHINA	531	550	97.5	1	0
2017-074B	JILIN-01-05	CHINA	526	545	97.5		
2017-074C	JILIN-01-06	CHINA	529	547	97.5		
2017-075A	YAOGAN-30 D	CHINA	598	602	35.0	1	0
2017-075B	YAOGAN-30 E	CHINA	596	603	35.0		
2017-075C	YAOGAN-30 F	CHINA	597	602	35.0		
2017-076A	COSMOS 2524	RUSSIA	901	910	67.2	1	0
2017-077A	LKW–1	CHINA	487	504	97.5	0	4
2017-078A	ALCOMSAT 1	ALGERIA	35775	35799	0.0	1	0
2017-079A	GALILEO 19 (2C5)	ESA	23298	23316	57.0	1	0
2017-079B	GALILEO 20 (2C6)	ESA	23171	23183	56.9		
2017-079C	GALILEO 21 (2C7)	ESA	23073	23096	56.9		
2017-079D	GALILEO 22 (2C8)	ESA	23156	23157	56.9		
2017-080A	DRAGON CRS-13	USA	402	406	51.6	0	2
2017-081A	SOYUZ MS-07	RUSSIA	402	406	51.6	1	0
2017-082A	GCOM-C	JAPAN	791	794	98.7	1	2
2017-082B	SLATS	JAPAN	458	628	98.3		
2017-083A	IRIDIUM 135	USA	664	681	86.6	0	0
2017-083B	IRIDIUM 138	USA	610	628	86.7		
2017-083C	IRIDIUM 116	USA	610	627	86.7		
2017-083D	IRIDIUM 130	USA	702	703	86.5		
2017-083E	IRIDIUM 151	USA	610	627	86.7		
2017-083F	IRIDIUM 134	USA	697	698	86.5		
2017-083G	IRIDIUM 137	USA	609	627	86.7		
2017-083H	IRIDIUM 141	USA	609	627	86.7		
2017-083J	IRIDIUM 153	USA	608	627	86.7		
2017-083K	IRIDIUM 131	USA	699	700	86.5		
2017-084A	LKW–2	CHINA	489	503	97.5	0	3
2017-085A	YAOGAN-30 G	CHINA	585	596	35.0	1	0
2017-085B	YAOGAN-30 H	CHINA	594	603	35.0		
2017-085C	YAOGAN-30 J	CHINA	604	611	35.0		
2017-086A	ANGOSAT 1	ANGOLA	35962	36117	0.1	2	5